

## Measurement of the longitudinal asymmetry of a charged particle bunch from the coherent synchrotron or transition radiation spectrum

R. Lai, U. Happek,\* and A. J. Sievers

*Laboratory of Atomic and Solid State Physics and Materials Science Center, Cornell University, Ithaca, New York 14853*

(Received 28 September 1994)

The shapes of submillimeter long electron bunches at the Cornell linear accelerator have been determined by measuring the coherent far-ir synchrotron and transition radiation spectrum produced by the charge distribution. With the aid of a Kramers-Kronig analysis of the spectral data, we show that the longitudinal bunch shape including the asymmetry can be accurately determined.

PACS number(s): 41.85.Qg, 41.60.-m, 41.75.Ht

In the past few years information on the bunch form factor, which is the modulus squared of the Fourier transform of the longitudinal charge distribution, has been obtained for short electron bunches from spectroscopic measurements of the coherent far-infrared spectrum [1–10]. It is assumed in the standard analysis method that the bunch is symmetric and hence the results cannot provide information about the longitudinal bunch asymmetry. In this paper we report on measurements of both synchrotron and transition far-ir radiation spectra produced by submillimeter electron bunches generated with the Cornell linear accelerator (linac) and then demonstrate that the complete longitudinal bunch shape including its asymmetry can be determined with the help of a previously proposed Kramers-Kronig procedure [11]. For experimental conditions similar to those used for injection into the Cornell synchrotron, both kinds of coherent spectra give the same largely asymmetric bunch shape.

Our experiments on the bunch length shape were performed at the 2856 MHz S-band linac that serves as an injector for the Cornell storage ring. It consists of a pulsed thermoionic triode gun, a two-stage subharmonic prebuncher, and a total of eight accelerator structures, capable of producing up to  $10^{11}$  electrons in a single microbunch with an energy of 300 MeV. Coherent synchrotron radiation was generated by the passage of the electrons through the field of a 0.44 T bending magnet. From the geometry of the vacuum chamber of the magnet we estimate that the synchrotron spectrum is unaffected by waveguide effects for frequencies higher than  $2\text{ cm}^{-1}$ . For the generation of transition radiation the bending magnet is turned off, and coherent radiation is produced by the passage of the electron bunch through the gold coated mirror. The radiation passes through a crystalline quartz window out of the vacuum chamber and is then collected by an off-axis parabolic mirror, and finally reflected off two additional flat mirrors into the spectrometer.

To analyze the spectrum of either types of radiation we use a polarizing grid Michelson spectrometer that can be remote controlled and is of rugged construction to allow for extended periods of experiment without further alignment. This type of spectrometer combined with Golay cell detec-

tors has the advantage of a fairly flat spectral response in the mm wavelength range. To correct for intensity fluctuations during the measurements, the spectrometer is equipped with an identical reference detector. The low frequency limit of the spectrometer, determined by diffraction losses and the finite aperture of the detectors, is about  $2\text{ cm}^{-1}$ ; the high frequency limit, determined by the grating constant of the polarizing wire beam splitters used in the instrument, is about  $50\text{ cm}^{-1}$ .

A measured spectrum of coherent synchrotron radiation is shown in Fig. 1(a). This spectrum has been obtained with single bunch operation at a repetition rate of 15 Hz, and  $2 \times 10^9$  electrons per bunch. The linac parameters (prebuncher phase and amplitude) are similar to the standard settings used for injection into the Cornell synchrotron. Under these conditions, the electrons are present in a single bunch, as confirmed experimentally by the lack of a cross correlation signal from electrons in adjacent rf cycles of the linac. The spectrum in Fig. 1(a) shows strong interference patterns, an indication of a structured bunch. The intensity grows rapidly with decreasing frequency, as expected for coherent radiation, and finally is suppressed below  $2\text{ cm}^{-1}$  due to the limited aperture and detector response. Figure 2(a) shows the measured coherent transition radiation spectrum under similar linac beam conditions.

To analyze these two sets of data in detail, the  $E$  field for the coherent part of the emission spectrum is written as [12]

$$\frac{\mathbf{E}_{\text{tot}}(\omega)}{\sqrt{N(N-1)}} = \mathbf{E}_{\text{eff}}(\omega) = \hat{S}(\omega)\mathbf{E}(\omega) \quad (1)$$

so that the effective  $E$  field at the detector is linearly related by  $\hat{S}(\omega)$  to the  $E$  field produced by an individual electron. This spectral function can be expressed as

$$\ln \hat{S}(\omega) = \ln \rho(\omega) + i\psi(\omega), \quad (2)$$

where  $\rho(\omega)$  is the modulus and  $\psi(\omega)$  is the phase factor. It can be shown that  $\hat{S}(\omega)$  can be analytically continued into the complex frequency plane and that the real and imaginary parts in Eq. (2) are related by the Kramers-Kronig relations [11,13]. If the form factor  $F(\omega) = S(\omega)S^*(\omega) = \rho^2(\omega)$  is measured at all frequencies, then the frequency dependent phase factor  $\psi(\omega)$  can be obtained through the following integration:

\*Present address: Department of Physics and Astronomy, University of Georgia, Athens, GA 30602-2451.

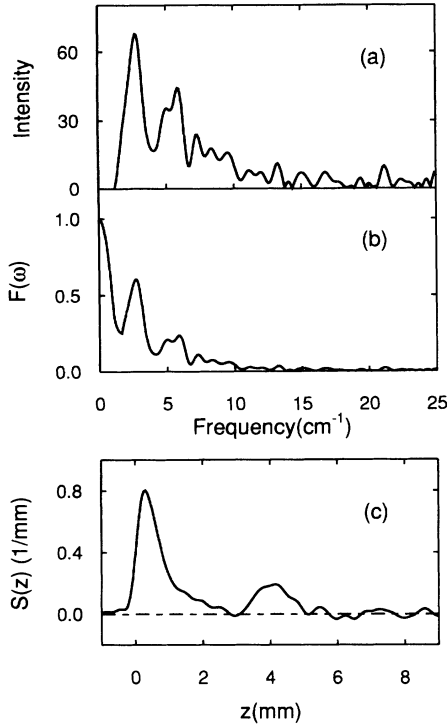


FIG. 1. Measured coherent synchrotron radiation spectrum and calculated longitudinal bunch shape. The experimental beam conditions are similar to those used for injection into the Cornell synchrotron. (a) The intensity spectrum in arbitrary units is shown as a function of frequency. (b) The data in (a) are divided by  $\omega^{2/3}$  then the low frequency asymptote is attached to the data between 0 and  $1.6 \text{ cm}^{-1}$  with  $F(0)$  normalized to 1. (c) The calculated longitudinal bunch shape versus distance.

$$\psi(\omega) = -\frac{2\omega}{\pi} \text{P} \int_0^\infty dx \frac{\ln[\rho(x)/\rho(\omega)]}{x^2 - \omega^2}. \quad (3)$$

With  $\psi(\omega)$  known the determination of the frequency dependence of the complex form factor is complete. The desired normalized bunch distribution function is [11]

$$S(z) = \frac{1}{\pi c} \int_0^\infty d\omega \rho(\omega) \cos\left[\psi(\omega) - \frac{\omega z}{c}\right]. \quad (4)$$

Since the experimentally measured spectrum cannot cover the entire frequency interval, asymptotic forms for  $F(\omega)$  are needed in both the low and high frequency region. As  $\rho(\omega)$  is an even function of  $\omega$ , the Taylor expansion of both  $\rho(\omega)$  and  $F(\omega)$  at low frequencies must be parabolic functions, hence  $F(\omega) \sim 1 - c\omega^2$  with positive  $c$ . To find the

high frequency asymptote we make use of the finite size of the electron bunch. Let its two end points be at  $z=0$ ,  $\sigma_z$  then  $S(0)=S(\sigma_z)=0$ . Integrating the spectral function by parts over the nonzero range gives

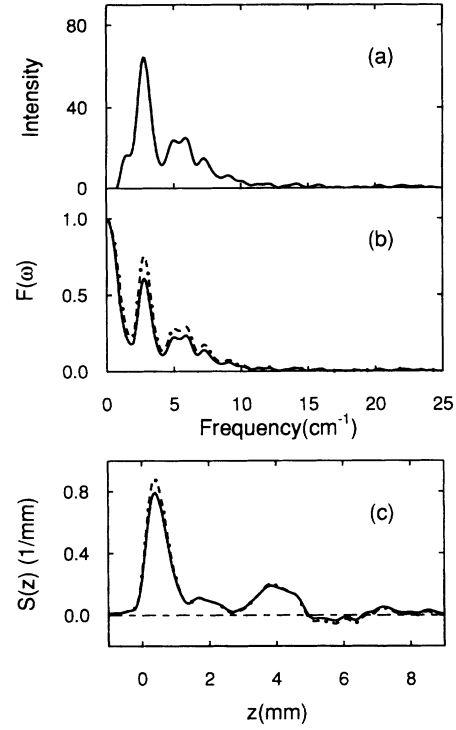


FIG. 2. Measured coherent transition radiation spectrum and calculated longitudinal bunch shape. The experimental linac beam conditions are similar to those used for injection into the Cornell synchrotron. (a) The intensity spectrum in arbitrary units as a function of frequency. (b) Two different zero frequency asymptotes between 0 and  $1.8 \text{ cm}^{-1}$  (solid and dot-dashed lines) are attached to the low frequency data in (a). (c) The calculated longitudinal bunch shape for both cases show that the relative height of  $F(0)$  plays only a small role in fixing the exact bunch shape.

$$\hat{S}(\omega) = \int_0^\infty dz S(z) e^{i(\omega/c)z}$$

$$= \frac{S(z)}{i \frac{\omega}{c}} e^{i(\omega/c)z} \Big|_0^{\sigma_z} - \frac{S'(z)}{\left(i \frac{\omega}{c}\right)^2} e^{i(\omega/c)z} \Big|_0^{\sigma_z} + \dots \quad (5)$$

Since the first term vanishes because of the boundary conditions, the leading term is proportional to  $\omega^{-2}$ ; hence for large  $\omega$ ,  $F(\omega)$  varies as  $\omega^{-4}$ . Once the phase factor  $\psi(\omega)$  is obtained, the bunch shape can be calculated from Eq. (4) with a triangular apodization function. The integration range is from 0 up to  $\omega_{\text{max}} = 25 \text{ cm}^{-1}$ , i.e., the range of measured spectra. The resolution of the bunch shape is therefore 0.35 mm.

To extract the bunch form factor from the spectrum in Fig. 1(a) we first correct the spectral distribution for the  $\omega^{2/3}$  frequency dependence of the single-electron emittance. Inspection of the resulting intensity versus the frequency data in Fig. 1(b) indicates that the high frequency asymptote represented by Eq. (5) can be readily matched to the data. Somewhat more care is required in analyzing the low frequency end of each spectrum since the intensity at the detector goes to zero while  $F(0)$  must equal one. For the spectrum with

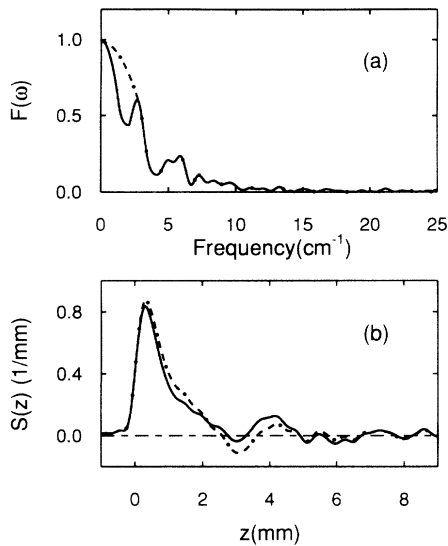


FIG. 3. Illustration of the influence of the low frequency asymptotic expansion of the form factor on the calculated bunch shape. The data are the same as given in Fig. 1. (a) The dot-dashed curve is attached at  $2.8 \text{ cm}^{-1}$  and the actual data below that frequency are ignored in one representation of  $F(\omega)$ . The solid curve shows the low frequency asymptote attached at  $2.1 \text{ cm}^{-1}$ . (b) The corresponding bunch shapes are shown. Note that for the dot-dashed curve the charge density is negative at about 3 mm, a nonphysical result. This feature is reduced as the attachment point is shifted to lower frequencies (solid curve). The shape of the first 2 mm of the bunch is only weakly effected by this shift.

the low frequency asymptotic attachment shown in Fig. 1(b), the longitudinal bunch shape shown in Fig. 1(c) is found. The main contribution is localized in the first 1 mm with a satellite feature appearing at 4 mm.

But how much of the resulting bunch shape is a function of the low frequency attachment? As long as the asymptotic attachment occurs at low frequencies, because of the intervening Fourier transform represented by Eq. (4), the uncertainties introduced by the low frequency details can only influence the corresponding bunch shape at large distances. The low frequency (and, hence, large distance) uncertainty comes from both the relative height of  $F(0)$  with regard to the measured spectrum and the frequency of the asymptotic attachment of two parameters. The normalization factor of the intensity spectrum can, in principle, be determined from the number of electrons in the bunch and the absolute intensity; however, a measurement of the absolute intensity has not yet been attempted. As we now show, neither the attachment frequency nor the relative size of  $F(0)$  have much effect on the bunch shape at small distances, the quantity of interest here.

To be more specific about the influence of the low frequency contribution of  $F(\omega)$ , we examine the resulting bunch shape for the same data but where the asymptote is attached at the lowest frequency peak and also at an intermediate frequency value compared to that given in Fig. 1(b). The composite spectra and the resulting bunch shapes are shown by the dot-dashed and solid lines in Figs. 3(a) and 3(b) respectively. Note that at large distances,  $\sim 3 \text{ mm}$ ,  $S(z)$  actually becomes significantly negative for the dot-dashed

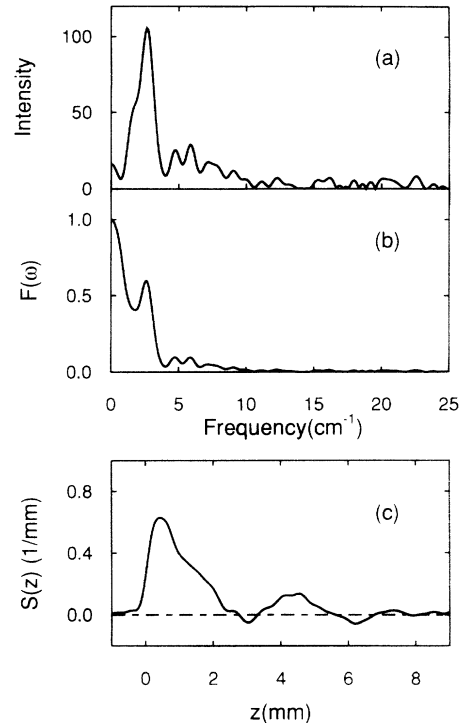


FIG. 4. Measured coherent synchrotron radiation spectrum with one prebuncher off and corresponding calculated longitudinal bunch shape. (a) The intensity spectrum is shown as a function of frequency. (b) The asymptotic form factor is attached to the data at  $1.8 \text{ cm}^{-1}$ . (c) The calculated longitudinal bunch shape is now much wider than in Figs. 1(c) or 2(c).

curve, a nonphysical result. The second composite spectrum with the low frequency asymptote attached at  $2.1 \text{ cm}^{-1}$  produces a reduced negative contribution to  $S(z)$  at this distance. The attachment at  $1.6 \text{ cm}^{-1}$  presented in Fig. 1(b) appears slightly better in terms of reducing the negative contributions to the bunch shape.

Since the single-particle emittance spectrum is flat for transition radiation, no frequency dependent correction to the data in Fig. 2(a) is required to make contact with the bunch form factor. In Fig. 2(b) the results for two different relative sizes of  $F(0)$  with respect to the intensity versus frequency profile (solid and dot-dashed lines) are shown. Both asymptotes are attached at  $1.8 \text{ cm}^{-1}$  and the resulting bunch shapes are nearly the same. Of the two parameters, the relative size of  $F(0)$  and the attachment frequency, the frequency has the largest influence on the bunch shape. Of course, to determine the exact bunch shape at large distances would require a more precise measurement at still lower frequencies. The important point here is that the main asymmetric peak in  $S(z)$  as determined from the synchrotron spectrum in Fig. 1(c) or by the transition radiation spectrum in Fig. 2(c) occurs at small distances ( $\sim 1 \text{ mm}$ ) and is essentially unaffected by the particular asymptotic expansion that is used. Very similar shapes  $S(z)$  are found by using both kinds of radiation for experimental conditions similar to those used for injection into the Cornell synchrotron.

Finally, to illustrate the influence of the prebunchers on the bunch length, one section of the prebuncher was turned

off and a set of synchrotron spectra recorded. Figure 4 shows the resulting far-ir spectrum and corresponding calculated bunch shape. The results show the expected behavior, that a longer asymmetric bunch results from less effective pre-bunching.

In conclusion, the Kramers-Kronig transform technique applied to the coherent far-ir spectrum produced by submillimeter charged particle bunches provides an alternative method for the measurement of the complete longitudinal shape. The only uncertainty in the shapes found here occurs at large distance because the lowest frequency radiation is

beyond the range of the detector system, an experimental problem. For shorter bunches like those recently reported [9], this complication will vanish since, in this case, the low frequency form factor asymptote can be attached at a much higher frequency where the experimental uncertainties are greatly reduced.

Conversations with M. Tigner are gratefully acknowledged. This work was supported by D.O.E. Grant No. DE-FG02-92-ER-4734 and ARO Grant No. DAAL03-92-G-0369.

- 
- [1] T. Nakazato *et al.*, Phys. Rev. Lett. **63**, 1245 (1989).
  - [2] Y. Shibata *et al.*, Nucl. Instrum. Methods Phys. Res. Sect. A **301**, 161 (1991).
  - [3] E. B. Blum, U. Happek, and A. J. Sievers, Nucl. Instrum. Methods Phys. Res. Sect. A **307**, 568 (1991).
  - [4] Y. Shibata *et al.*, Phys. Rev. A **44**, R3445 (1991).
  - [5] U. Happek, E. B. Blum, and A. J. Sievers, Phys. Rev. Lett. **67**, 2962 (1991).
  - [6] K. Ishi *et al.*, Phys. Rev. A **43**, 5597 (1991).
  - [7] Y. Shibata *et al.*, Phys. Rev. A **45**, R8340 (1992).
  - [8] Y. Shibata *et al.*, Phys. Rev. E **49**, 785 (1994).
  - [9] P. Kung, H.-C. Lihn, H. Wiedeman, and D. Bocek, Phys. Rev. Lett. **73**, 967 (1994).
  - [10] Y. Shibata *et al.*, Phys. Rev. E **50**, 1479 (1994).
  - [11] R. Lai and A. J. Sievers, Phys. Rev. E **50**, R3342 (1994).
  - [12] J. S. Nodvick and D. S. Saxon, Phys. Rev. **96**, 180 (1954).
  - [13] F. Wooten, *Optical Properties of Solids* (Academic, New York, 1972).